Glycoconj J (2015) 32:643–653
DOI 10.1007/s10719-015-9612-8

ORIGINAL ARTICLE

Preparation and characterization of heparin hexasaccharide library with *N*-unsubstituted glucosamine residues

Qun Tao Liang[1] · Jia Yan Du[1] · Qing Fu[1] · Jiang Hui Lin[1] · Zheng Wei[1]

Received: 21 May 2015 / Revised: 15 July 2015 / Accepted: 24 July 2015 / Published online: 15 August 2015

Abstract The rare N-unsubstituted glucosamine ($GlcNH_3^+$) residues in heparan sulfate (HS) have important biological and pathophysiological roles. Therefore, the ability to chemically generate a series of oligosaccharides, which have a similar structure to the naturally-occurring, $GlcNH_3^+$ - containing oligosaccharides from HS, would greatly contribute to investigating their natural role in HS. In this study, a hexasaccharide library that possess $GlcNH_3^+$ residues were prepared from the chemical modification of the fully sulfated dp6. Chemical reaction conditions were optimized to generate different pattern of $GlcNH_3^+$ - containing oligosaccharides, then the structure of the library was detected by high-performance liquid chromatography-ion trap/time-of-flight mass spectrometry (LC/MS-ITTOF) analysis. EIC/MS and MS^2 analysis showed different fragmentation patterns of dp6s with different $GlcNH_3^+$ residues. This provides a foundation for further identification and quantification of $GlcNH_3^+$ - oligosaccharides by mass spectrum analysis.

Keywords Heparin · Hexasaccharide · *N*-unsubstituted disaccharide · LC-MS-ITTOF

Abbreviations

CyPB	Cyclophilin-B
DMSO	Dimethyl sulfoxide
dp	Degree of polymerization (corresponds to the number of monosaccharide units, *i.e.* dp2 is a disaccharide)
EIC	Extracted ion chromatography
GAGs	Glycosaminoglycans
GlcA	β-D-glucuronic acid
GlcNAc	β-D-*N*-acetylglucosamine
$GlcNH_3^+$	β-D-*N*-unsubstituted glucosamine
GlcNS	β-D-*N*-sulfoglucosamine
HS 3-OST	Heparan sulfate 3-O-sulfotransferases
HS	Heparan sulfate
HSV	Herpes simplex virus
IdoA	α-L-iduronic acid
IPRP-LC-ITTOF	Ion-pair reversed-phase liquid chromatography-ion trap/time-of-flight mass spectrometry
LMWH	Low molecular weight heparin
NDST	*N*-deacetylase/*N*-sulfotransferase
PTA	n-pentylamine
RT	Retention time
SAX-HPLC	Strong anion-exchange HPLC
SE-HPLC	Size-exclusion HPLC

Introduction

Heparin and HS have important biological activities in developmental processes, angiogenesis, blood coagulation, cell adhesion, and tumour metastasis [1–4]. These biological functions are related to their structural diversity and ability to interact with cell surfaces and extracellular

Electronic supplementary material The online version of this article (doi:10.1007/s10719-015-9612-8) contains supplementary material, which is available to authorized users.

✉ Zheng Wei
zheng0wei@hotmail.com

[1] Institute of Glycobiochemistry, National Engineering Research Centre of Chemical Fertilizer Catalyst, Fu Zhou University, Fu Zhou 350002, People's Republic of China

proteins, and structures of these GAGs are significant determinants of their binding interactions [5, 6].

HS and heparin share a common biosynthetic pathway, being initially synthesized as repeating disaccharides of alternating β1→4 glucuronic acid (GlcA) and α1→4 *N*-acetylglucosamine (GlcNAc) [7–10]. This non-sulfated precursor is then modified by co-ordinated *N*-deacetylation / *N*-sulfation of GlcNAc residues by *N*-deacetylase / *N*-sulfotransferase enzymes (NDST), forming *N*-sulfoglucosamine (GlcNS) *via* an *N*-unsubstituted glucosamine ($GlcNH_3^+$) intermediate. Subsequently, further modifications occur, *i.e.* C5-epimerization of GlcA to α1→4 iduronic acid (IdoA), 2-*O*-sulfation of hexuronic acid (primarily IdoA), 6-*O*-sulfation of GlcNS or GlcNAc, and lastly the rare, but functionally important, 3-*O*-sulfation of GlcNS by 3-O-sulfotransferases (HS 3-OST).

The rare $GlcNH_3^+$ residues implicated in important cell-biological and pathophysiological phenomena [7, 11–14] are also now particularly hot subjects in the pharmaceutical industry. Additional $GlcNH_3^+$ residues can be generated by thermal stress and autoclave sterilization of heparin. This can modify, and compromise, the highly specific, endogenous antithrombin III-binding sites, resulting in a decrease in the anticoagulant potency that is the main medicinal application of heparin [15, 16]. Recently its tumour invasion and metastasishas raised interest. The chemically synthetic HS-tetrasaccharides containing $GlcNH_3^+$ residues, GlcAβ1-4 $GlcNH_3^+$ (6-*O*-sulfate) α1-4 GlcA β1-4 $GlcNH_3^+$ (6-*O*-sulfate), inhibited heparanase activity and suppressed invasion of breast cancer cells *in vitro* [17]. Therefore, the generation of the $GlcNH_3^+$ containing heparin/HS oligosaccharide library is useful for their functional study.

It has become clear that the $GlcNH_3^+$ residue exists in mature HS/heparin, which may be due to an occasional interruption of the NDST-mediated, catalytic linkage between *N*-deacetylation and re-*N*-sulfation, thereby trapping the intermediate $GlcNH_3^+$. In general, the content of $GlcNH_3^+$ in HS species is low, but variable across different tissues. It mostly ranges from 0.2 to 4 % of disaccharide units [18–22], but reaches a moderately high 12 % in bovine kidney HS [19]. The location of $GlcNH_3^+$ residues and the nature of their surrounding sequences might contribute to their enzyme susceptibility, antibody recognition and protein interactions. Previously, we demonstrated that the various heparinase enzymes have differential specificities toward $GlcNH_3^+$ residues [19], and a series of heparin/HS oligosaccharides containing internal $GlcNH_3^+$ residues were generate by heparinases [23]. Because of the limitation of specificity of heparinases, we further generated a full range of oligosaccharides processing different locations of $GlcNH_3^+$ by chemical modification [24], with potential use in development of structure sequencing and functional study.

Mass spectroscopy is now becoming a much more useful tool for the structural analysis of heparin/HS oligosaccharides because of its high detection sensitivity and molecular specificity [25–27]. MS/MS^n of heparin/HS oligosaccharides can produce information-rich glycosidic and cross-ring product ions which can be used to determine the sites of acetylation or sulfation, therefore leading the structural determination [28]. In particular, LC-MS clearly has the potential now to sequence most oligosaccharides, especially with the recent development of a computational framework for dealing with the complex data generated [29]. Recently, we developed a novel method for sequencing $GlcNH_3^+$ containing oligosaccharides by a combination of HNO_2 deployment, SE-HPLC, and LC-MS-ITTOF, which offered possibilities to identify the structure of chemical modified oligosaccharides [24].

In this study, we optimized the chemical reaction of de-*N*-sulfation of oligosaccharide to prepare a full range of heparin dp6s with different positions of $GlcNH_3^+$ residues, for potential use in structural studies by LC-MS-ITTOF.

Materials and methods

Materials

An enzymatically depolymerized low molecular weight heparin (LMWH, Innohep) was obtained from Leo Laboratories Ltd (Princes Risborough, Bucks, UK). Twelves HS disaccharide standards were purchased from Iduron (Manchester, UK). Bio-Gel P-10 (fine grade) was obtained from Bio-Rad Laboratories (Hemel Hempstead, Herts., UK). ProPac PA-1 HPLC column was obtained from Dionex (Camberley, Surrey, UK).

Heparinase I (Flavobacterium heparinum; heparin lyase EC 4.2.2.7) and heparin II (F. heparinum; no EC number assigned) were purchased from Sigma Aldrich (St. Louis, Mo., USA). Calcium acetate (AR), sodium acetate (AR), potassium acetate (AR) were all obtained from Sinopharm Chemical Reagent Co. Ltd (Shanghai, China). Bovine serum albumin (96 %) was purchased from Aladdin Reagent Co. Ltd (Shanghai, China). Acetonitrile was provided by Merck KGaA (Darmstadt, Germany). Ammonium bicarbonate (AR), sodium chloride, hydrochloric acid (AR), Amberlite IR-120(H^+ form), pyridine (>99.9 %), dimethyl sulfoxide (DMSO, AR), formic acid (98 %), trifluoroacetic acid (GC), sodium hydroxide (≥98 %) and amylamine (PTA, 99 %) were all purchased from Sigma Aldrich (Heysham, Lancs, UK). All HPLC solutions were prepared using MilliQ (Millipore, Watford, Herts., UK) ultra pure water.

Preparation of fully sulfated heparin hexasaccharide (dp6)

The fully sulfated dp6, comprised of three tri-sulfated disaccharides, was prepared as previously described [23]. Briefly, heparin dp6 was isolated from low molecular weight heparin (Innohep) by Bio-Gel P-10 chromatography. The fully sulfated dp6 was then resolved from the individual dp6 mixtures, respectively, by strong anion-exchange HPLC (SAX-HPLC).

Partial de-*N*-sulfation of dp6

The partial de-*N*-sulfation of dp6 was prepared as previously described [24]. The modification procedure consisting of three major steps starts with the fully sulfated dp6 (see Fig. S1). The pyridinium salt of dp6 was obtained by passage through an Amberlite IR-120 (H^+ form) column and titration of the resulting protonated form with pyridine. The pyridinium salt was then treated with 95 % DMSO, 5 % water at 27–30 °C for 20 min followed by extensive dialysis and freeze-drying.

Optimization of partially de-*N*-sulfated dp6 reaction

In order to optimize the partial de-*N*-sulfated reaction, the pyridinium salt was treated with 95 % DMSO, 5 % water at 25 °C ranging from 25 to 45 min. In addition, the reaction time was maintained for 30 min, but the reaction temperature was varied between 20 and 45 °C. The products were then separated and analysed by SAX-HPLC as described below.

Strong anion-exchange HPLC

SAX-HPLC separation of dp6 fractions was performed on an Agilent Technologies-1200 HPLC with an analytical ProPac PA-1 column (4.0×250 mm). Samples were applied in 1 ml of water adjusted to pH 3.5 with HCl, washed with pH3.5 water for 2 min, and then eluted using a biphasic, linear gradient of NaCl, pH 3.5 from 0 to 0.8 M (2.1–7.1 min) and then 0.8 to 1.5 M (7.1–47.1 min), at a flow rate of 1 ml/min. The eluent was monitored by on-line absorbance at 232 nm.

LC/MS – ITTOF analysis

A hybrid ion trap/time-of-flight mass spectrometer coupled to a high-performance liquid chromatography system (LC/MS-ITTOF) (Shimadzu Corp., Kyoto, Japan) was used to analyse partially de-*N*-sulfated dp6s. The liquid chromatography system was equipped with a binary gradient pump (LC-20 AD), autosampler (SIL-20AC), degasser (DGU-20A3), photodiode array detector (SPD-M20A), communication base module (CBM-20A) and a column oven (CTO-20AC). Separations were performed by ion-pair reversed-phase chromatography (IPRP-HPLC) on a 3.5 μm Eclipse Plus C18 column (2.1× 100 mm) at a flow rate of 0.2 ml/min at 35 °C. Both eluent A (water) and eluent B (75 % acetonitrile *v/v*) contained 15 mM PTA ion pairing reagent and were adjusted to pH 8.8 with formic acid. The linear elution gradient was 5 to 100 % B over 20 min. The photodiode array detection was performed from 190 to 800 nm. In order to investigate the fragmentation pattern of dp6 oligosaccharides, the samples were dissolved in 10 % acetonitrile (*v/v*) and infused to the mass spectrometer at a flow rate of 0.2 ml/min. The product ions are reported using the Domon and Costello nomenclature [30].

The mass spectrometer was equipped with an electrospray ionization (ESI) source and was operated in the negative mode. Mass spectroscopic analyses were carried out on a full-scan mass spectrometer with a mass range of 200–1800 m/z. Liquid nitrogen was used as the nebulizing gas at a flow of 1.5 L/min. The curved desolvation line and heat block temperatures were both 100 °C. The interface voltages were set at −3.5 kV, and the detector voltage was 1.6 kV. The IT and TOF area vacuums were maintained at 1.8e - 002 Pa and 1.6e - 004 Pa, respectively. External mass calibration was carried out prior to data acquisition using direct infusion of a reference standard from 150 to 2100 m/z. The reference standard consisted of 0.25 ml/L trifluoroactic acid and approx 0.1 g/L sodium hydroxide. The flow rate of the infusion pump was 0.2 ml/min. All calculated mass errors were less than 5 ppm after mass calibration with the reference standard. The product ions which have 10^5 of ESI-MS spectrum intensity were automatically selected as precursor ions for MS^2 analysis. Argon was used as collision gas. The ion accumulation time was set at 100 msec. Samples dissolved in 10 % acetonitrile were directly infused to the mass spectrometer at a flow rate of 0.2 ml/min.

Results and discussion

It has been demonstrated that the sulfated disaccharide sequence IdoA (2S)-$GlcNH_3^+$(±6S) is a target for the HS 3-OST-3 enzyme, which generates binding sites for the gD glycoprotein of HSV-1 [31] and for CyPB [32]. This disaccharide could be primarily located with the highly sulfated domains of HS. Therefore, highly sulfated oligosaccharides containing potentially sulfated $GlcNH_3^+$ residues in different positions could be particularly valuable substrates for testing protein binding activities and also enzyme susceptibilities.

Preparation of fully sulfated heparin hexasaccharide (dp6)

LMWH have already been partially degraded by heparinase I, which introduces an unsaturated bond between C4 and C5 of the non-reducing terminal uronate residues. LMWH was separated by Bio-Gel P-10 size-exclusion chromatography, and

the dp6 fraction was further purified by SAX-HPLC on a ProPac column (Fig. S2). Three major peaks were obtained, labelled as dp6A, dp6B and dp6C respectively. Dp6C has the longest retention time which suggests that it has a highly sulfated pattern, as SAX-HPLC separation is based on charge density differences. The disaccharide analysis of dp6C showed that only one major disaccharide peak, ΔHexA(2S)-GlcNS(6S), was obtained (data not shown), indicating that dp6C contains three tri-sulfated-dp2, ΔHexA(2S)-GlcNS(6S)-HexA(2S)-GlcNS(6S)-HexA(2S)-GlcNS(6S). The combination of the above result and the IPRP-HPLC-MS analysis (in the section of IPRP-LC /MS-ITTOF analysis) shows that dp6C fraction mainly contains highly sulfated oligosaccharide with nine sulfate groups, however, the absolute purity of dp6C can only be guaranteed by additional analyse, *e.g.* NMR.

Preparation of N-unsubstituted dp6 library

In this study, a full range of dp6 containing a variety of content and sequence of $GlcNH_3^+$ residues were prepared by partial de-*N*-sulfation, and their sequencing were determined by combination of HNO_2 deployment and LCMS-ITTOF as described at our previous paper [24]. As shown in Fig. 1, three species of dp6s containing 1 to 3 $GlcNH_3^+$ residues were obtained. Dp6-1a and dp6-1b were the isomers containing 1 $GlcNH_3^+$ residues. Dp6-1a contains two species which had a $GlcNH_3^+$ residue at either end of the oligosaccharides, while dp6-1b has a $GlcNH_3^+$ residue locating in the central disaccharide. In our previous study, a series of oligosaccharides with internal $GlcNH_3^+$ residues were generated by de-*N*-sulfation of heparin followed by heparinase I digestion [23]. However as the limitation of heparinases, the oligosaccharides with a $GlcNH_3^+$ residue at both ends of the chain were not generated by heparinases degradation. Therefore, through controlling the reaction conditions, these oligosaccharides could be successfully obtained by directly partial de-*N*-sulfation of dp6. Further, these could mimic highly sulfated domains with a rare $GlcNH_3^+$ in native HS, which provide a larger range of $GlcNH_3^+$ residues containing oligosaccharides for functional study.

In contrast, three species, dp6-2a, dp6-2b and dp6-2c, containing two $GlcNH_3^+$ residues in different positions were generated. Our previous sequencing results have shown that dp6-2a with two $GlcNH_3^+$ residuesis located in the central and reducing terminal positions, while dp6-2b is located at the reducing and non-reducing termini. On the other hand, dp6-2c was thus determined to have two $GlcNH_3^+$ residues present in the central and non-reducing terminal positions. These results suggested that the whole permutation and combination of $GlcNH_3^+$ residues in dp6 were obtained by this partial de-*N*-sulfation. It is possible that after re-acetylation, these could be converted into oligosaccharides that then more closely model mixed *N*-acetylated/ *N*-sulfated domains of HS.

The SAX-HPLC profile (see Fig. S3) has shown that dp6 isomers possess different proportion, of which dp6-1b, dp6-2c and dp6-3 were major products, and dp6-1a, dp6-2a and dp6-2b were minor ones. As the reaction yields are different in each species, the conditions of de-*N*-sulfation need to be optimized to increase the amounts of minor isomers, suitable for the structural and functional studies.

Optimization of partial de-*N*-sulfation of dp6

Partial de-*N*-sulfation procedure consisting of three major steps starts with the fully sulfated dp6 (Fig. S1). The de-*N*-sultated pattern is varied with the reaction temperature and time. In order to compare the degree of de-*N*-sultation, different temperatures and reaction times were chosen for reaction. The modified mixtures were further separated by SAX-HPLC, and the relative proportion was determined by their corresponding UV peak areas.

Different partial de-*N*-sulfation was carried out at 18, 20, 25, 30, 35, 40 and 45 °C, respectively, for 30 min. The relative proportions of the modified dp6 species are summarized in Table 1. As shown in all temperatures, the major products of modification were dp6-3, dp6-2c and dp6-1b. The relative proportion of the fraction dp6-3 rise along with the increased temperature, and reached 83.72 % at 45 °C. The content of dp6C decreased when the temperature became higher, showing no detection at 40 °C. In dp6-1a and dp6-1b isomers, their highest content were obtained between 20 and 25 °C, which correspond to 30 % and 5–7 %, respectively. In contrast, three dp6-2 species had the highest relative content between 25 and 35 °C. Dp6-2c contained 25–28 %, while dp6-2a and dp6-2b were about 4–9 %. These data suggested that abundant dp6 with a variety of content and sequence of $GlcNH_3^+$ residues were obtained between 25 and 30 °C in the same reaction.

The influencing factors of the de-*N*-sulfation time were analysed at 25 °C for 25, 30, 35, 40 and 45 min respectively. As shown in Table 2, the relative proportions of the modified dp6s have dramatic differences in reaction time. Dp6-1a, dp6-1b and dp6-2a showed relatively high content for a 25–30 min reaction, while dp6-2b and dp6-2c also showed a high reaction at 35–40 min.

These results showed that de-*N*-sulfation of dp6 under suboptimal conditions does not lead to random, proportionate loss of *N*-sulfates at available positions. The relative higher and equal content of dp6-1b and dp6-2c were detected in the reaction products, indicating that de-*N*-sulfation has initially and preferentially occurred at an internal position, than at non-reducing termini. The dp6s containing $GlcNH_3^+$ residues at reducing terminal position (dp6-1a, dp6-2a and dp6-2b) were shown to have a lower yield in chemical reaction, suggesting that loss of *N*-sulfate from the reducing terminal hexosamine

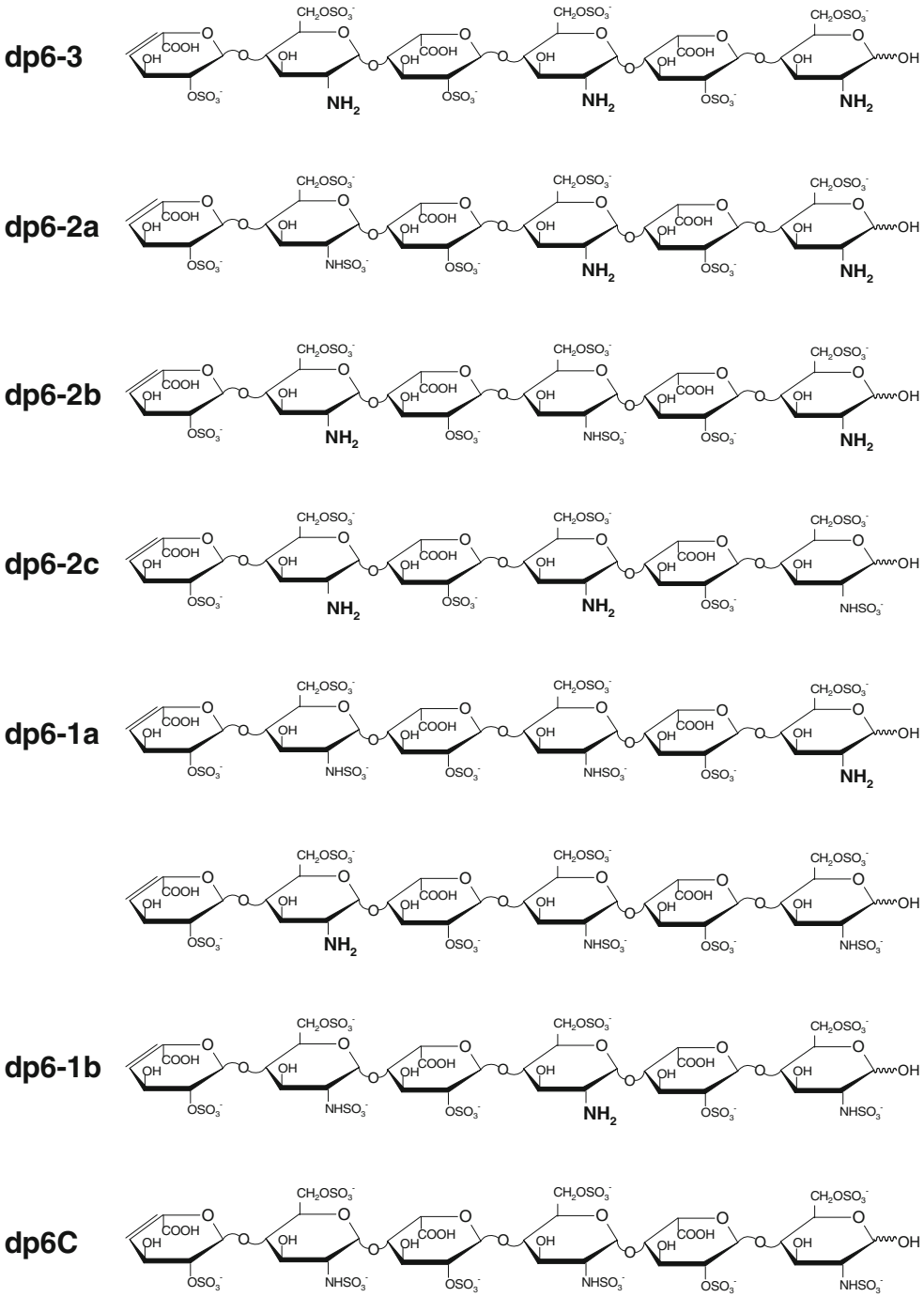

Fig. 1 The structures of dp6s containing different $GlcNH_3^+$ residues. Dp6-3 contains three $GlcNH_3^+$ residues. Dp6-2a, dp6-2b and dp6-2c are isomers possessing two, while dp6-1a and dp6-1b contain one $GlcNH_3^+$ residue. The dp6C is the fully sulfated one

occurs much more slowly and/or only after prior loss of the non-reducing terminal N-sulfate (presumably reflecting the markedly different conformations and chemical environments at these two positions). This study first showed the regular pattern of *N*-sulfate loss during the de-*N*-sulfation of oligosaccharide, which provided theory evidence for generating longer size $GlcNH_3^+$ residues containing oligosaccharides.

The six dp6 species with $GlcNH_3^+$ residues were individually pooled and structurally analyzed further by ion-pair reversed-phase liquid chromatography (IPRP-LC) coupled with ion trap / time-of-flight mass spectrometry (ITTOF), *i.e.* IPRP-LC/MS-ITTOF.

IPRP-LC /MS-ITTOF analysis

IPRP-LC coupled with online MS detection is a promising technique for the analysis of heparin oligosaccharides with minimal sample preparation. This system achieves a highly efficient separation, together with only a limited sulfate group loss during MS analysis [33], allowing to detect the intact

Table 1 Effect of temperature in partial de-N-sulfation of dp6s

	Relative contents of dp6s (%)						
	dp6-3	dp6-2a	dp6-2b	dp6-2c	dp6-1a	dp6-1b	dp6C
18 °C	17.07	0.53	8.57	21.22	3.03	18.38	31.20
20 °C	18.88	4.14	5.54	21.27	6.65	30.55	12.96
25 °C	23.67	4.42	5.77	25.30	5.10	27.40	8.35
30 °C	29.97	5.20	7.99	28.31	3.37	19.26	5.91
35 °C	54.07	1.04	9.80	24.49	0.83	7.63	2.15
40 °C	68.33	0.00	6.39	20.41	0.00	4.87	0.00
45 °C	83.72	0.00	3.81	12.48	0.00	0.00	0.00

The pyridinium salt of the fully sulfated dp6 was treated with 95 % DMSO, 5 % water for 30 min at different temperatures. The values of the relative proportions for each fraction were calculated using the area of peaks in SAX-HPLC (as described in Fig. S3)

molecular ions and obtain accurate molecular weight measurements, from which oligosaccharides with different degrees of $GlcNH_3^+$ residues can be identified. Due to the fragility of sulfate group in MS analysis, the buffer system and the mass spectrometer settings were optimized by using fully sulfated dp6 (dp6C) to minimize the sulfate loss during the analysis. Sample analysis utilized both mass spectra and extracted ion chromatography (EIC) profiles. The MS profiles are shown in Fig. 2, the formulas of molecular ions corresponding to the ion peaks in Fig. 2 are shown in Table S1, S2, S3 and S4, respectively. As shown in the MS data of dp6C (Fig. 2a), two major ion peaks appeared at *m/z* 1125.7643 and 1082.2139 with two negative charges, corresponding to $[M+6PTA-2H]^{2-}$ and $[M+5PTA-2H]^{2-}$. The other ion peaks were shown in Table S1, the frequency of all ion peaks in MS profile was calculated by their corresponding EIC peak areas. Three molecular ions with sulfate loss, $[M-3SO_3+5PTA-2H]^{2-}$, $[M-SO_3+4PTA-2H]^{2-}$, $[M-SO_3+5PTA-2H]^{2-}$ were detected, in which shown only 2.04 % of total amount of ion peaks. These molecular ions have the same elution position as the other PTA adducts in EIC profile (data not shown), suggesting that the minor sulfate losses appear in MS ion source.

Six dp6s with $GlcNH_3^+$ residues were analysed by the same MS conditions of dp6C. The results of one $GlcNH_3^+$ residue containing isomers dp6-1a and dp6-1b were shown in Fig. 2b and c, and Table S2. Three major peaks, corresponding to PTA adducts (from 3 to 5 PTAs) were detected in both dp6-1a and dp6-1b. Very small amounts of the naked molecular ion $[M-3H]^{3-}$ with three negative charges was obtained. The sulfate loss molecular ions were detected both in dp6-1a and dp6-1b with 1.52 and 3.91 % in total amounts, respectively. In our previous work [24], the dp6-1a fraction was sequenced by a combination of HNO_2 cleavage, SE-HPLC and IPRP-LC-ITTOF, which showed that dp6-1a is actually a mixture of two different dp6s with one free amino group at either the RE or the NRE. As the $GlcNH_3^+$ residues are located at either end of the oligosaccharides, presumably their "mirror image" similarities in conformation and linear charge distribution make them difficult to resolve by the IPRP-HPLC-MS analysis system.

In contrast, the major ion peaks in dp6-2a, dp6-2b and dp6-2c were PTA adducts (see Table S3), however, the sulfate losses in three samples were significantly different in the MS analysis. No sulfate loss was detected in dp6-2a, while 3.15 and 10.81 % of sulfate loss ion peaks were obtained in dp6-2b and dp6-2c, respectively. The sulfation degree and $GlcNH_3^+$ residues content of dp6-2a, dp6-2b and dp6-2c are exactly the same; however the significant difference of sulfate losses appearing in MS analysis suggesting that the location of $GlcNH_3^+$ residues might affect the PTA adduction to the oligosaccharides due to the density difference of positive charges.

On the other hand, the MS profile of dp6-3 has shown that beside PTA adducts, a high proportion of naked molecular ion $[M-2H]^{2-}$, about 17.14 %, appeared. The sulfate loss content, about 11.07 %, is higher than other $GlcNH_3^+$ residues containing dp6, suggesting that higher positive charges might increase the steric hindrance of PTA adduction.

Table 2 Effect of reaction time for partial de-N-sulfation of dp6s

	Relative contents of dp6s (%)						
	dp6-3	dp6-2a	dp6-2b	dp6-2c	dp6-1a	dp6-1b	dp6C
25 min	21.00	4.75	6.22	21.15	5.20	26.44	15.24
30 min	25.44	3.90	6.54	24.43	4.27	25.86	9.57
35 min	36.82	1.14	12.63	28.00	1.45	16.78	3.17
40 min	49.38	1.92	10.73	30.77	0.97	6.23	0.00
45 min	78.89	0.00	3.04	18.08	0.00	0.00	0.00

The pyridinium salt of the fully sulfated dp6 was treated with 95 % DMSO, 5 % water at 25 °C with different reaction times. Values of the relative proportions for each fraction were calculated using the area of peaks in SAX-HPLC (as described in Fig. S3)

Fragmentation pattern of dp6s

Tandem mass spectrometry (MS/MS^n) have been explored by a number of researchers as tools for the structural analysis of GAGs, as it can produce information-rich glycosidic and cross-ring product ions which can be used to determine the sites of acetylation or sulfation [28]. Because MS/MS^n analysis produces abundant structurally useful fragments, dp6-3, dp6-2c and dp6-1b were selected to investigate fragmentation pattern of dp6s with different $GlcNH_3^+$ residues, for the further potential structure analysis by MS.

Dp6 samples were dissolved in 10 % acetonitrile and directly infused to the mass spectrometer. The MS spectra of dp6s are shown in Figs. 3, 4, and 5. Ionization of dp6-3

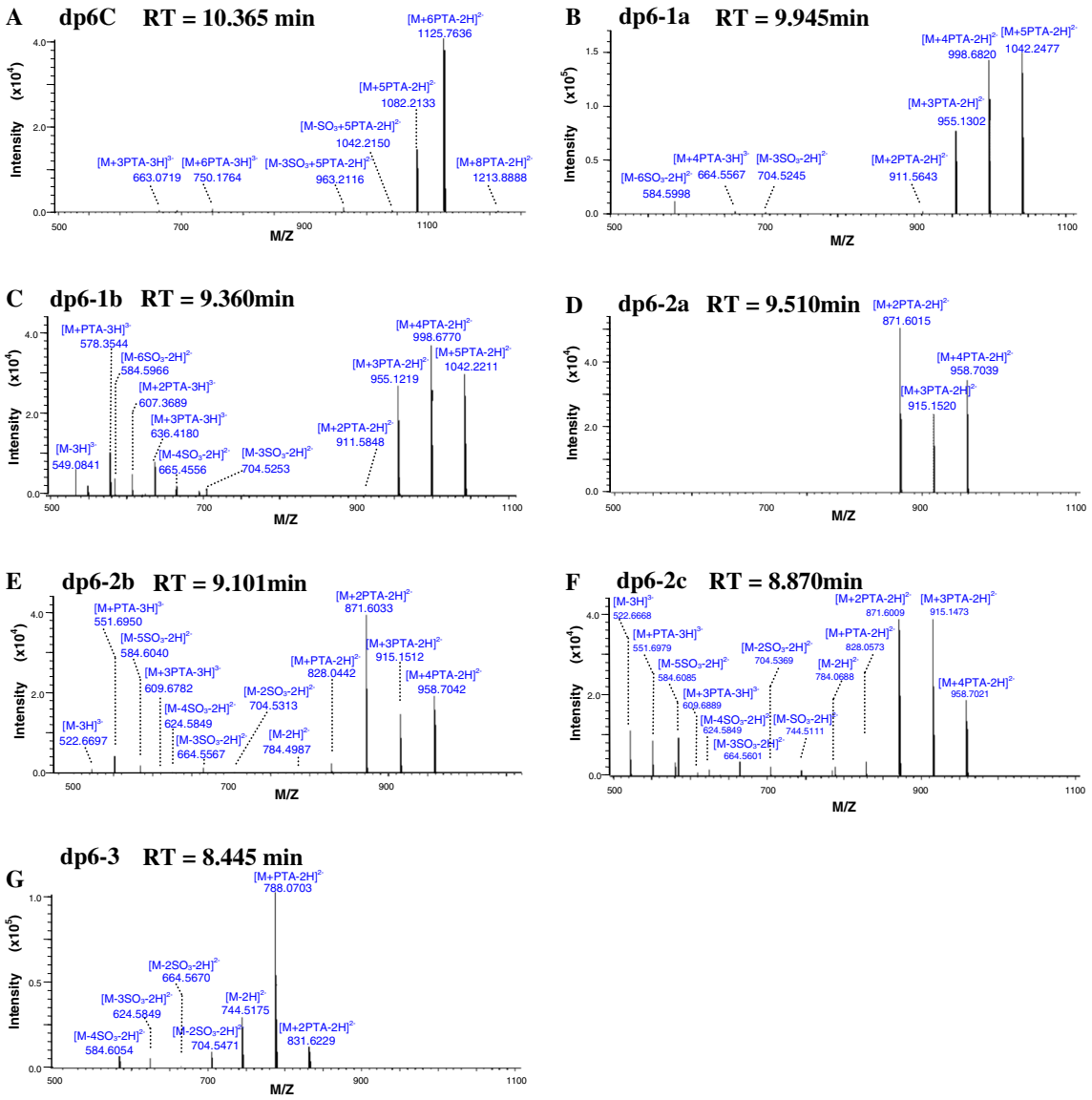

Fig. 2 IPRP-LC-ITTOF analysis of dp6s with different $GlcNH_3^+$ residues. **a** is a MS spectrum of fully sulfated Dp6C. **b** and **c** are those of dp6-1a and dp6-1b which contain one $GlcNH_3^+$ residue, respectively. **d**–**f** are the spectra of dp6-2a, dp6-2b and dp6-2c, respectively. The spectrum of dp6-3 with three $GlcNH_3^+$ residues is shown in (**g**). The molecular ions corresponding to the peaks in MS spectra are summarized in Table S1, S2, S3 and S4

(Fig. 3a), dp6-2c (Fig. 4a) and dp6-1b (Fig. 5a) results in the formation of four charge states, 5-, 4-, 3- and 2-, in which the abundancy of charged ions were different in each dp6 sample, *e.g.* 4- ion in dp6-3 and 5- ions in dp6-2c and dp6-1b are the most abundant in the spectrum. This probably indicates the presence of charge-charge repulsion limitation of each of the charged ions [34]. The ESI mass spectra has shown that the charged naked molecular ions are the major products, with other fragment ions produced from neutral loss of a small molecule (SO_3, H_2O, CH_2O or CO_2H), glycosidic and cross-ring cleavages are in low abundance. In order to further investigate the full fragmentation of three dp6s, the molecular ions with 10^5 of intensity in ESI-MS were automatically selected as precursor ions for MS^2 analysis. From the product ions in ESI-MS and MS^2 spectra, the possible fragmentation patterns of three dp6s were summarized.

ESI-MS and MS^2 analysis of dp6-3 are shown in Fig. 3. MS spectrum (Fig. 3a) revealed a four negative charged product ion at *m/z* 303.7718 corresponding to $[Y_5\text{-}2H_2O\text{-}2H]^{4-}$, indicating that the glycosidic cleavages Y_5 exist in MS analysis of oligosaccharide. Five product ions derived from cross-ring cleavage with different abundances were detected, and their corresponding fragmentations are shown in Fig. 3d in black dotted lines. As shown in Fig. 3a, double negative charged ions of $[^{1,4}X_3\text{-}2SO_3\text{-}H_2O\text{-}H]^{2-}$ (*m/z* 331.7755) and $[^{1,5}X_3\text{-}SO_3\text{-}2H]^{2-}$ (*m/z* 351.7642) were obtained, indicating that $^{1,4}X_3$ and $^{1,5}X_3$ fragmentations appeared in the second glucuronic acid residues (from the non-reducing end) of

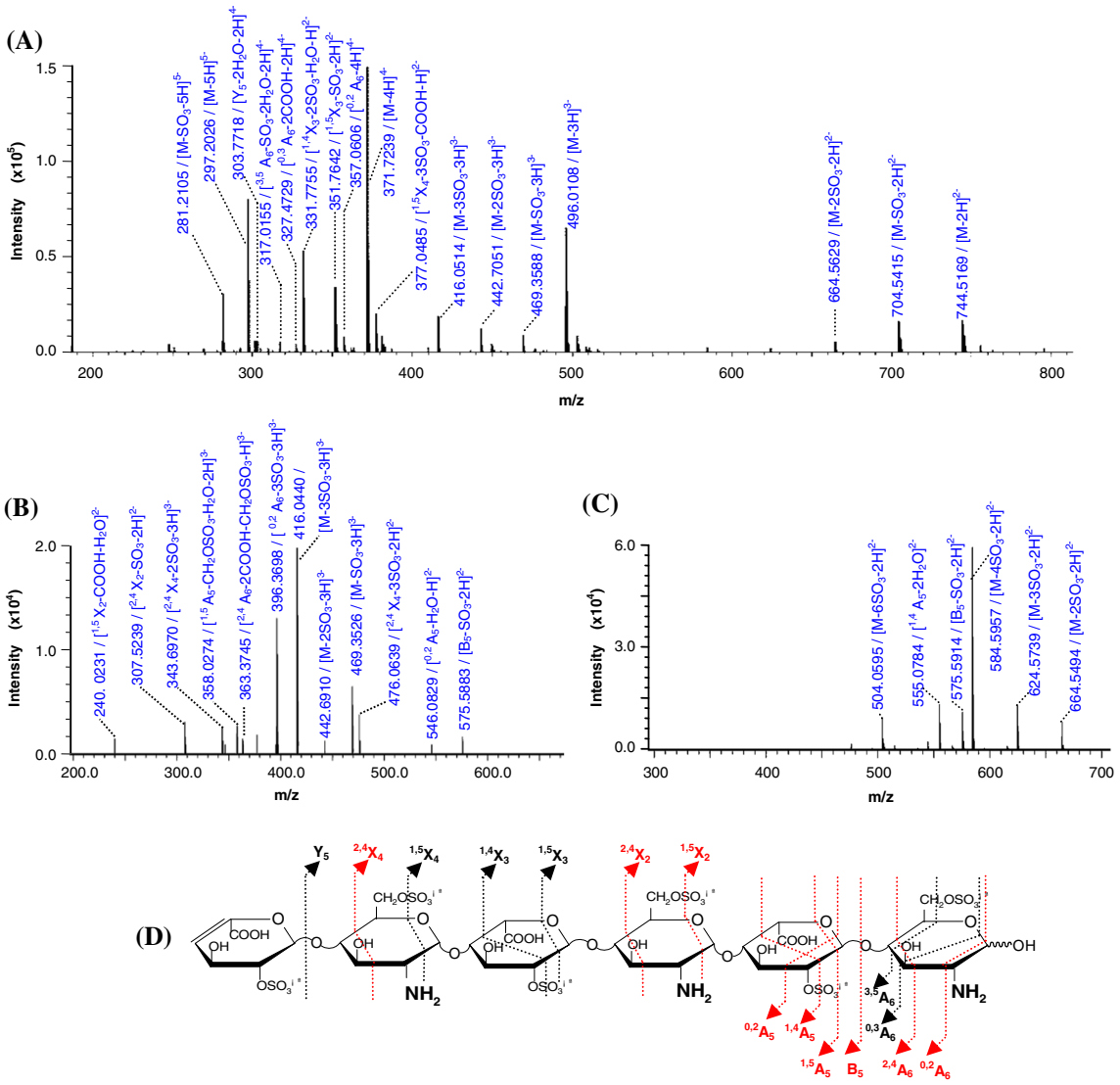

Fig. 3 ESI-MS and MS^2 analysis of dp6-3 with three $GlcNH_3^+$ residues. The generated molecular ions in ESI-MS spectrum (**a**) and their corresponding fragmentations labelled as *black dotted lines* (**d**) are summarized. As representative data, the MS^2 spectra of $[M-3H]^{3-}$ (**b**) and $[M-SO_3-2H]^{2-}$ (**c**) are selectively shown. The observed fragmentations from MS^2 analysis are summarized as *red dotted lines* in panel (**d**)

dp6-3. The $[^{1,5}X_4\text{-}3SO_3\text{-}COOH\text{-}H]^{2-}$ (at *m/z* 377.0485) production corresponding to $^{1,5}X_4$ fragmentation in the first glucosamine residue of oligosaccharide was revealed. In addition, two 4- charged ion peaks corresponding to $[^{3,5}A_6\text{-}SO_3\text{-}2H_2O\text{-}2H]^{4-}$ (at *m/z* 317.0155) and $[^{0,3}A_6\text{-}2COOH\text{-}2H]^{4-}$ (at *m/z* 327.4729) were present, suggesting $^{3,5}A_6$ and $^{0,3}A_6$ fragmentations exist in the third glucosamine residues of dp6-3. The product ions with 10^5 intensity in ESI-MS were automatically selected as precursor ions for MS^2 analysis. Herein, two representative MS^2 spectra of $[M-3H]^{3-}$ and $[M-SO_3-2H]^{2-}$ precursor ions were selectively shown. As shown in MS^2 spectra (Fig. 3b, c), a product ion $[B_5\text{-}SO_3\text{-}2H]^{2-}$ at *m/z* 575.5 was detected, suggesting that the glycosidic cleavages B_5 exist. In contrast, besides X_4 and A_6, X_2 and A_5 cross-ring cleavage while not being detected in the ESI-MS spectrum exist in MS^2 analysis. As shown in spectra $[^{1,5}X_2\text{-}COOH\text{-}H_2O]^{2-}$ and $[^{2,4}X_2\text{-}SO_3\text{-}2H]^{2-}$, product ions corresponding to $^{1,5}X_2$ and $^{2,4}X_2$ fragmentations in the second glucosamine residue of oligosaccharide were present. Again, $^{0,2}A_6$ and $^{2,4}A_6$ cleavages were present in the third glucuronic acid residues of oligosaccharide. In summary, two glycosilic cleavages (Y_5, B_5) and thirteen cross-ring cleavages including X_4, X_3, X_2, A_5 and A_6 fragmentation were present in the ESI-MS/MS^2 analysis of dp6-3.

In contrast, ESI-MS/MS^2 analysis of dp6-2c (Fig. 4a, b and c) showed that the two glycosilic cleavages (Y_5, B_5) and nine cross-ring cleavages including X_4, X_3, A_5 and A_6 fragmentations were detected, while no X_2 fragmentation in the second glucosamine residue of oligosaccharide was found to exist. Like dp6-3, Y_5 (from $[Y_5\text{-}4H]^{4-}$ in Fig. 4a) and B5 (from

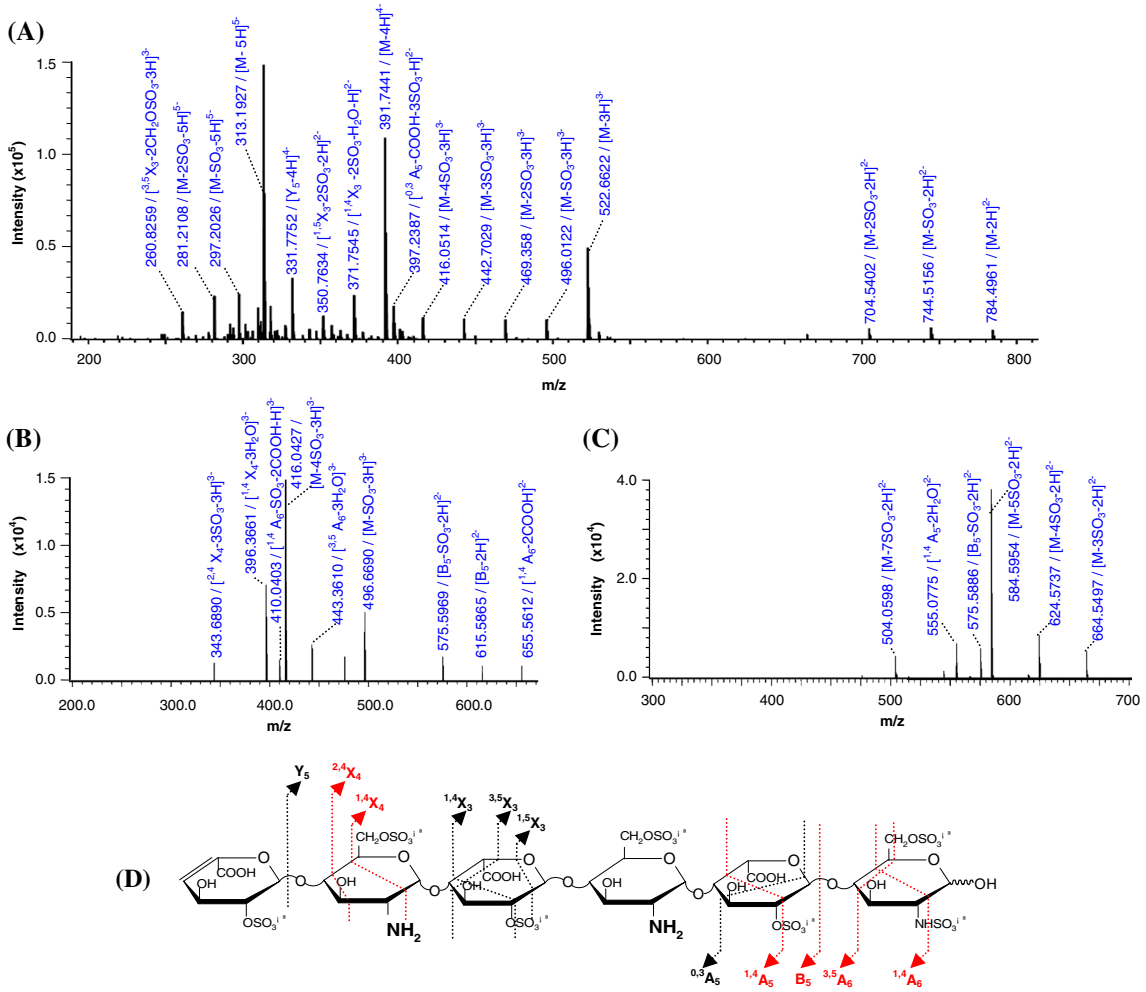

Fig. 4 ESI-MS and MS^2 analysis of dp6-2c with two $GlcNH_3^+$ residues. The generated molecular ions in ESI-MS spectrum (**a**) and their corresponding fragmentations labelled as *black dotted lines* (**d**) are summarized. As representative data, the MS^2 spectra of $[M-3H]^{3-}$ (**b**) and $[M-2SO_3-2H]^{2-}$ (**c**) are selectively shown. The observed fragmentations from MS^2 analysis are summarized as *red dotted lines* in panel (**d**)

$[B_5\text{-}2H]^{2-}$ in Fig. 4b) were revealed in dp6-2c. $^{2,4}X_4$ (from $[^{2,4}X_4\text{-}3SO_3\text{-}3H]^{3-}$ at *m/z* 343.6890) and $^{1,4}X_4$ (from $[^{1,4}X_4\text{-}3H_2O]^{3-}$ at *m/z* 396.3661) cleavages were obtained in the MS^2 spectra (Fig. 4b), while three X_3 cleavages ($^{1,4}X_3$, $^{3,5}X_3$ and $^{1,5}X_3$) were shown in ESI-MS spectrum (Fig. 4a). In addition, $^{0,3}A_5$, $^{1,4}A_5$, $^{3,5}A_6$ and $^{1,4}A_6$ framentations were revealed in dp6-2c.

Furthermore, only one glycosilic cleavage (Y_5) and six cross-ring cleavages including X_3, A_4, A_5 and A_6 fragmentations were detected in dp6-1b. Compared to dp6-3 and dp6-2c, only Y_5 glycosilic cleavage exists in dp6-1b, but no B_5 fragmentation was found. Meanwhile, $^{3,5}A_4$ fragmentation in the second glucosamine residue of oligosaccharide was only detected in dp6-1b.

The above ESI-MS and MS^n results provided different fragmentation patterns of dp6s with different $GlcNH_3^+$ residues. The dp6 with higher $GlcNH_3^+$ residues revealed more cross-ring cleavage patterns, suggesting that higher positive charges might make the ring more fragile, presumably reflecting the markedly different conformations and chemical environments at these positions, which results in different dissociation of dp6s in MS. This would be useful for further structural identification and quantification of $GlcNH_3^+$ - oligosaccharides by mass spectrum.

Summary

A full range of dp6s containing 1 to 3 $GlcNH_3^+$ residues with different sequences were prepared by a single chemical modification by controlling the reaction conditions. The optimization of partial de-*N*-sulfation demonstrated that the priority of removing *N*-sulfate was from internal hexosamine first, and then from the non-reducing terminal and finally from the reducing terminal. This de-*N*-sulfation pattern might provide theory evidence for generating larger

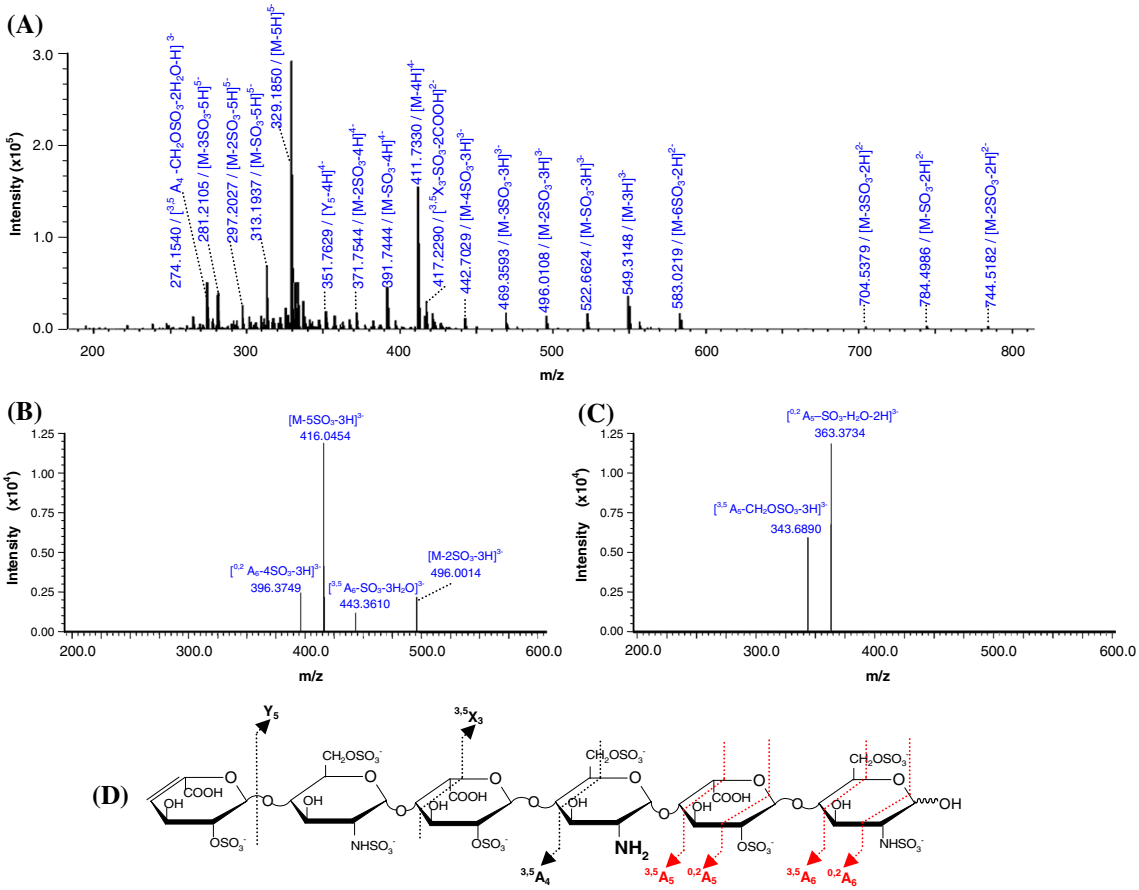

Fig. 5 ESI-MS and MS^2 analysis of dp6-1b with a $GlcNH_3^+$ residues. The generated molecular ions in ESI-MS spectrum (**a**) and their corresponding fragmentations labelled as *black dotted lines* (**d**) are summarized. As representative data, the MS^2 spectra of $[M\text{-}SO_3\text{-}3H]^{3-}$ (**b**) and $[M\text{-}4SO_3\text{-}3H]^{3-}$ (**c**) are selectively shown. The observed fragmentations from MS^2 analysis are summarized as *red dotted lines* in panel (**d**)

$GlcNH_3^+$ residues containing oligosaccharides, which give structures that mimic natural $GlcNH_3^+$-containing sequences in HS/heparin. ESI-MS/MS^2 analysis showed that dp6s with higher $GlcNH_3^+$ residues revealed more cross-ring cleavages, and that the glycosidic and cross-ring cleavage patterns were different between three dp6s. These results demonstrated that MS would be useful tool for further identification and quantification of the $GlcNH_3^+$ -oligosaccharide isomers which are derived from chemical modification, and also for $GlcNH_3^+$-HS oligosaccharides possessing important biological functions. Overall, these $GlcNH_3^+$ residues containing dp6s could be valuable for testing protein binding activities in vitro and also enzyme susceptibilities, which could lead to a greater understanding of the biological roles of $GlcNH_3^+$ residues in HS/heparin.

Acknowledgments This work was supported by Grants 20773023 and 21343013 from National Natural Science Foundation of China.

References

1. Couchman, J.R.: Syndecans: proteoglycan regulators of cell-surface microdomains? Nat. Rev. Mol. Cell Biol. **4**, 926–937 (2003)
2. Liu, D., Shriver, Z., Venkataraman, G., El Shabrawi, Y., Sasisekharan, R.: Tumor cell surface heparan sulfate as cryptic promoters or inhibitors of tumor growth and metastasis. Proc. Natl. Acad. Sci. U. S. A. **99**, 568–573 (2002)
3. Perrimon, N., Bernfield, M.: Specificities of heparan sulphate proteoglycans in developmental processes. Nature **404**, 725–728 (2000)
4. Robinson, C.J., Stringer, S.E.: The splice variants of vascular endothelial growth factor (VEGF) and their receptors. J. Cell Sci. **114**, 853–865 (2001)
5. Kamimura, K., Koyama, T., Habuchi, H., Ueda, R., Masu, M., Kimata, K., Nakato, H.: Specific and flexible roles of heparan sulfate modifications in Drosophila FGF signaling. J. Cell Biol. **174**, 773–778 (2006)
6. Kreuger, J., Spillmann, D., Li, J.P., Lindahl, U.: Interactions between heparan sulfate and proteins: the concept of specificity. J. Cell Biol. **174**, 323–327 (2006)
7. Esko, J.D., Lindahl, U.: Molecular diversity of heparan sulfate. J. Clin. Invest. **108**, 169–173 (2001)

8. Lindahl, U., Kusche-Gullberg, M., Kjellén, L.: Regulated diversity of heparan sulfate. J. Biol. Chem. **273**, 24979–24982 (1998)
9. Esko, J.D., Selleck, S.B.: Order out of chaos: assembly of ligand binding sites in heparan sulfate. Annu. Rev. Biochem. **71**, 435–471 (2002)
10. Casu, B., Lindahl, U.: Structure and biological interactions of heparin and heparan sulfate. Adv. Carbohydr. Chem. Biochem. **57**, 159–206 (2001)
11. Cheng, F., Svensson, G., Fransson, L.-Å., Mani, K.: Non-conserved, S-nitrosylated cysteines in glypican-1 react with N-unsubstituted glucosamines in heparan sulfate and catalyze deaminative cleavage. Glycobiology **11**, 1480–1486 (2012)
12. Shukla, D., Liu, J., Blaiklock, P., Shworak, N.W., Bai, X., Esko, J.D., Cohen, G.H., Eisenberg, R.J., Rosenberg, R.D., Spear, P.G.: A novel role for 3-O-sulfated heparan sulfate in herpes simplex virus 1 entry. Cell **99**, 13–22 (1999)
13. Liu, J., Shriver, Z., Pope, R.M., Thorp, S.C., Duncan, M.B., Copeland, R.J., Raska, C.S., Yoshida, K., Eisenberg, R.J., Cohen, G., Linhardt, R.J., Sasisekharan, R.: Characterization of a heparan sulfate octasaccharide that binds to herpes simplex virus type 1 glycoprotein D. J. Biol. Chem. **277**, 33456–33467 (1997)
14. Liu, J., Shriver, Z., Blaiklock, P., Yoshida, K., Sasisekharan, R., Rosenberg, R.D.: Heparan sulfate D-glucosaminyl 3-O-sulfotransferase-3A sulfates N-unsubstituted glucosamine residues. J. Biol. Chem. **274**, 38155–38162 (1999)
15. Fu, L., Li, L., Cai, C., Li, G., Zhang, F., Linhardt, R.J.: Heparin stability by determining unsubstituted amino groups using HILIC-MS. Anal. Biochem. **461**, 46–48 (2014)
16. Beaudet, J.M., Weyers, A., Solakyildirim, K., Yang, B., Takieddin, M., Mousa, S., Zhang, F., Linhardt, R.J.: Impact of autoclave sterilization on the activity and structure of formulated heparin. J. Pharm. Sci. **100**, 3396–3404 (2011)
17. Nadanaka, S., Purunomo, E., Takeda, N., Tamura, J.I., Kitagawa, H.: Heparan sulfate containing unsubstituted glucosamine residues: biosynthesis and heparanase-inhibitory activity. J. Biol. Chem. **289**, 15231–15243 (2014)
18. Shi, X., Zaia, J.: Organ-specific heparan sulfate structural phenotypes. J. Biol. Chem. **284**, 11806–11814 (2009)
19. Wei, Z., Lyon, M., Gallagher, J.T.: Distinct substrate specificities of bacterial heparinases against N-unsubstituted glucosamine residues in heparan sulfate. J. Biol. Chem. **280**, 15742–15748 (2005)
20. Rees, M.D., Pattison, D.I., Davies, M.J.: Oxidation of heparan sulphate by hypochlorite: role of N-chloro derivatives and dichloramine-dependent fragmentation. Biochem. J. **391**, 125–134 (2005)
21. Westling, C., Lindahl, U.: Location of N-unsubstituted glucosamine residues in heparan sulfate. J. Biol. Chem. **277**, 49247–49255 (2002)
22. Toida, T., Yoshida, H., Toyoda, H., Koshiishi, I., Imanari, T., Hileman, R.E., Fromm, J.R., Linhardt, R.J.: Structural differences and the presence of unsubstituted amino groups in heparan sulphate from different tissues and species. Biochem. J. **322**, 499–506 (1997)
23. Wei, Z., Deakin, A.J., Blaum, B.S., Uhrín, D., Gallagher, J.T., Lyon, M.: Preparation of heparin / heparan sulfate oligosaccharides with internal N-unsubstituted glucosamine residues for functional studies. Glycoconj. J. **28**, 525–535 (2011)
24. Liang, Q.T., Xiao, X.X., Lin, J.H., Wei, Z.: A new sequencing approach for N-unsubstituted heparin/heparan sulfate oligosaccharides. Glycobiology **25**(7), 714–725 (2015)
25. Huang, R., Liu, J., Sharp, J.S.: An approach for separation and complete structural sequencing of heparin/heparan sulfate-like oligosaccharides. Anal. Chem. **85**, 5787–5795 (2013)
26. Wolff, J.J., Chi, L., Linhardt, R.J., Amster, I.J.: Distinguishing glucuronic from iduronic acid in glycosaminoglycan tetrasaccharides by using electron detachment dissociation. Anal. Chem. **79**, 2015–2022 (2007)
27. Schenauer, M.R., Meissen, J.K., Seo, Y.J., Ames, J.B., Leary, J.A.: Heparan sulfate separation, sequencing, and isomeric differentiation: ion mobility spectrometry reveals specific iduronic and glucuronic scid-containing hexasaccharides. Anal. Chem. **81**, 10179–10185 (2009)
28. Shi, X., Huang, Y., Mao, Y., Naimy, H., Zaia, J.: Tandem mass spectrometry of heparan sulfate negative ions: sulfate loss patterns and chemical modification methods for improvement of product ion profiles. J. Am. Soc. Mass Spectrom. **23**, 1498–1511 (2012)
29. Hu, H., Huang, Y., Mao, Y., Yu, X., Xu, Y., Liu, J., Zong, C., Boons, G.J., Lin, C., Xia, Y., Zaia, J.: A computational framework for heparan sulfate sequencing using high-resolution tandem mass spectra. Mol. Cell. Proteomics **13**, 2490–2502 (2014)
30. Domon, B., Costello, C.E.: A systematic nomenclature for carbohydrate fragmentations in FAB-MS/MS spectra of glycoconjugates. Glycoconj. J. **5**, 397–409 (1988)
31. Liu, J., Shriver, Z., Pope, M., Thorp, S.C., Duncan, M.B., Copeland, R.J., Sasisekharan, R.: Characterization of a heparan sulfate octasaccharide that binds to herpes simplex virus type 1 glycoprotein D. J. Biol. Chem. **277**, 33456–33467 (2002)
32. Vanpouille, C., Deligny, A., Delehedde, M., Denys, A., Melchior, A., Liénard, X., Lyon, M., Mazurier, J., Fernig, D.G., Allain, F.: The heparin/heparan sulfate sequence that interacts with cyclophilin B contains a 3-O-sulfated N-unsubstituted glucosamine residue. J. Biol. Chem. **282**, 24416–24429 (2007)
33. Doneanu, C.E., Chen, W.B., Gebler, J.C.: Analysis of oligosaccharides derived from heparin by ion-pair reversed-phase chromatography/mass spectrometry. Anal. Chem. **81**, 3485–3499 (2009)
34. Zaia, J., Costello, C.E.: Tandem mass spectrometry of sulfated heparin-like glycosaminoglycan oligosaccharides. Anal. Chem. **75**, 2445–2455 (2003)